Multi-frequency polarimetry of complete samples of extragalactic radio sources

– Radio source populations and cosmological perspectives –

ALMA
EUROPEAN ARC
ALMA Regional Centre || Italian

Dr. Marcella Massardi
INAF-IRA & Italian ARC

Prof. Loretta Gregorini
INAF-IRA

Vincenzo Galluzzi
INAF-OATs & IRA

Aeneas
Advanced European Network of E-infrastructures for Astronomy with the SKA

ISTITUTO NAZIONALE DI ASTROFISICA INAF

Outlines

- Context: AGN unified model and open problems

  for extragalactic radio sources (ERS) selected at 20 GHz
- State-of-art of the art on statistical polarimetric studies
- ATCA and ALMA observations
- Analysis:
  - **Spectral classification**
  - **Linear polarization**
  - **Polarization angle**
  - Circular polarization
  - Variability
  - Peculiar objects
  - **Source counts**
- Synergies:
  - **ERS foreground forecast for CMB studies**
  - **Perspectives for SKA: the T-RECS simulation**
- Conclusions

AGN unified view

(Antonucci 1993, Urry & Padovani 1995)

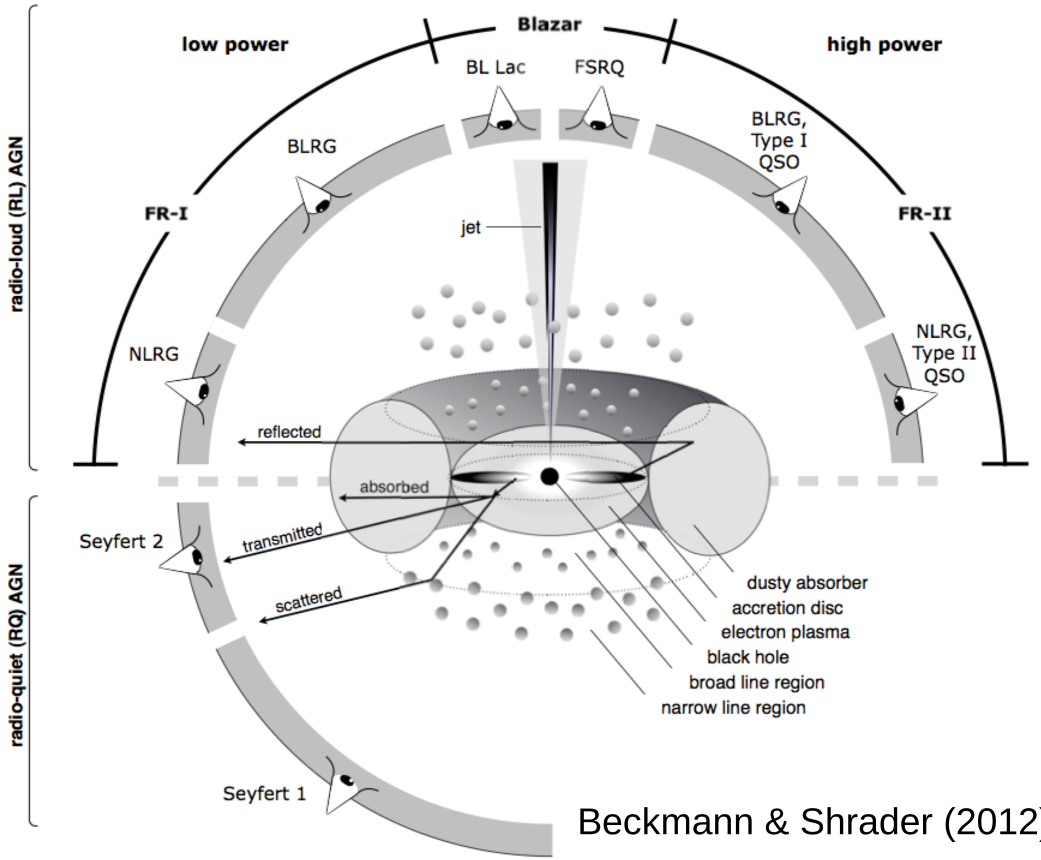

Beckmann & Shrader (2012)

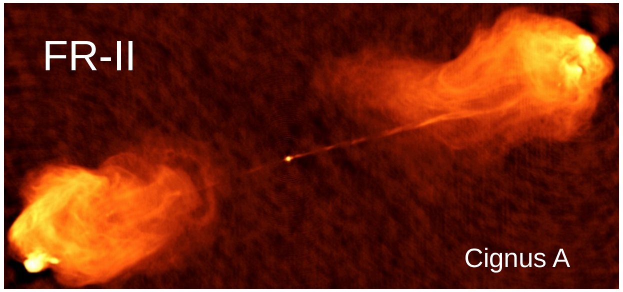

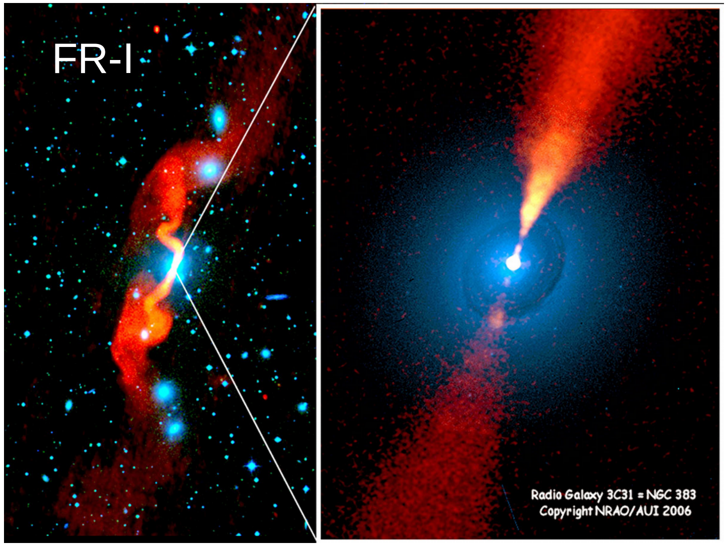

- The radio sky for frequencies > 20 GHz and bright flux density (> 0.1 Jy) is dominated by blazars, i.e. FSRQs and BL Lacs.
- Blazars constitute a peculiar class of AGNs appearing compact unless you go to mas resolutions

AGN unified view

(Antonucci 1993, Urry & Padovani 1995)

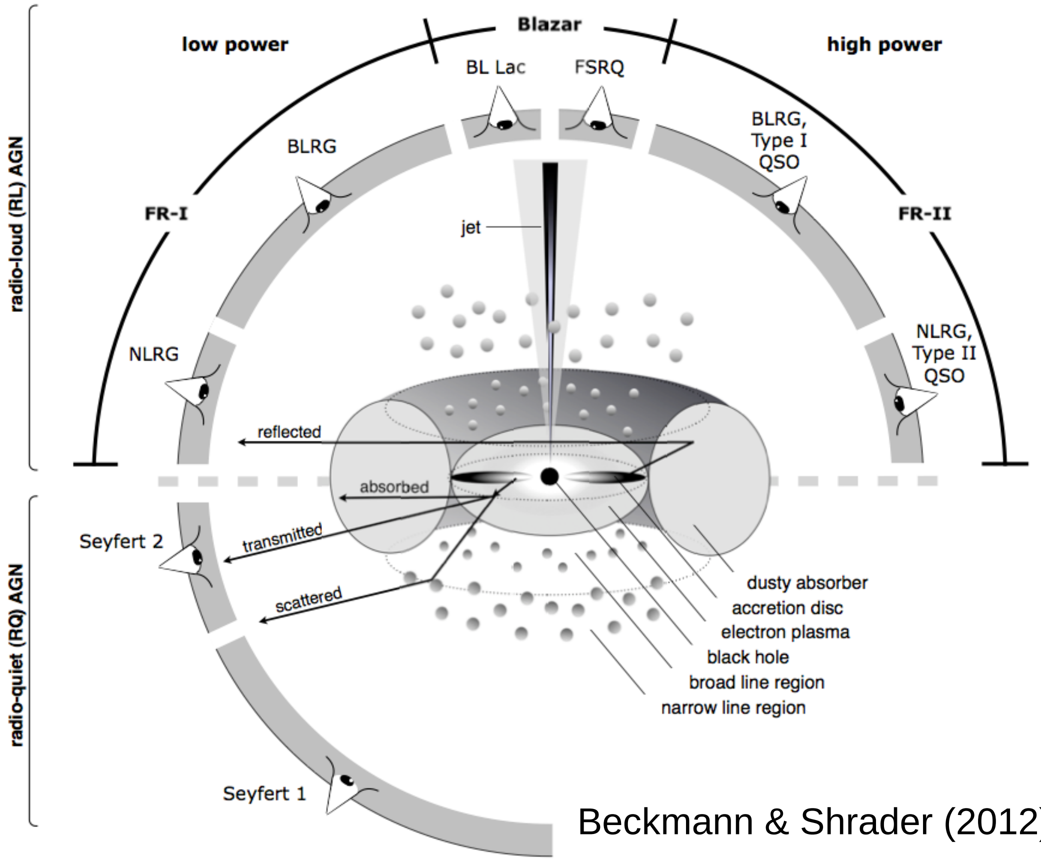

Beckmann & Shrader (2012)

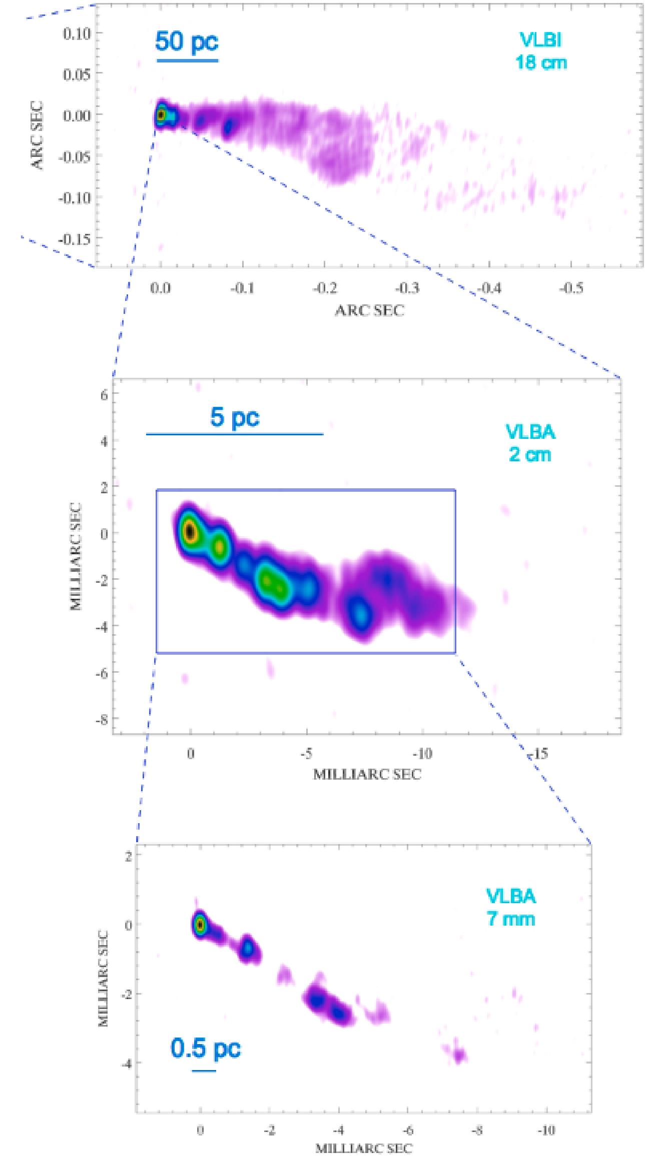

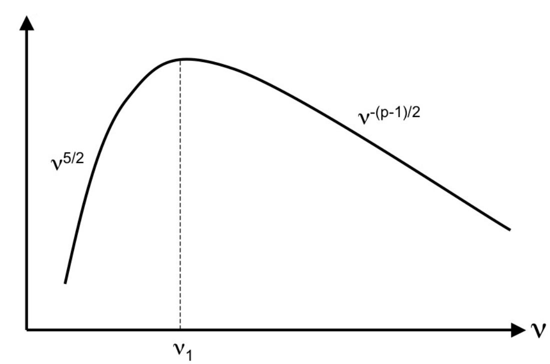

- The radio sky for frequencies > 20 GHz and bright flux density (> 0.1 Jy) is dominated by blazars, i.e. FSRQs and BL Lacs.
- Blazars constitute a peculiar class of AGNs appearing compact unless you go to mas resolutions

Open questions in AGN jets physics

- Where the **jet** is originated and what is the **powering mechanism** (direct extraction from the SMBH, Blandford & Znajek 1977 and/or from the accretion flow, Blandford & Payne 1982)?
- What about the **strength** and **topology** of the **magnetic field**, **its role in the jet launching** and its **collimation**, as well as in **acceleration processes** along the jet?
- What are the **particle acceleration mechanisms** (which bring particles up to relativistic energies) along the jet?
- Synchrotron signals show an **inverse Compton signature**. What about the origin (synchrotron self-Compton, SSC, and/or external photons, e.g from the accretion disk, CMB or EBL ones)?
- What is the **structure of the jet**, i.e. a faster spine (with bulk Lorentz factor $\Gamma = 10-20$) surrounded by a slower layer (with $\Gamma \approx 5$)?
- How other **AGN features influence the jet emissions** (e.g., NLR or BLR clouds)?
- What is the **jet composition**, e.g. a pure electron-positron plasma or a proton-electron plasma?

Cosmological motivations

- Contaminant for CMB angular power spectrum
- Too many young objects paradox (cfr. GPS, HFP)
- Indentify calibrators for cosmological studies (e.g. CMB, CPR)

In this case the statistical approach allow to model radio source population (completeness is a crucial element) both in total intensity and polarization

- So far models at cosmological window frequencies (70-100 GHz) are affected by large uncertainties due to extrapolations from lower frequencies (< 20 GHz) or from total intensity

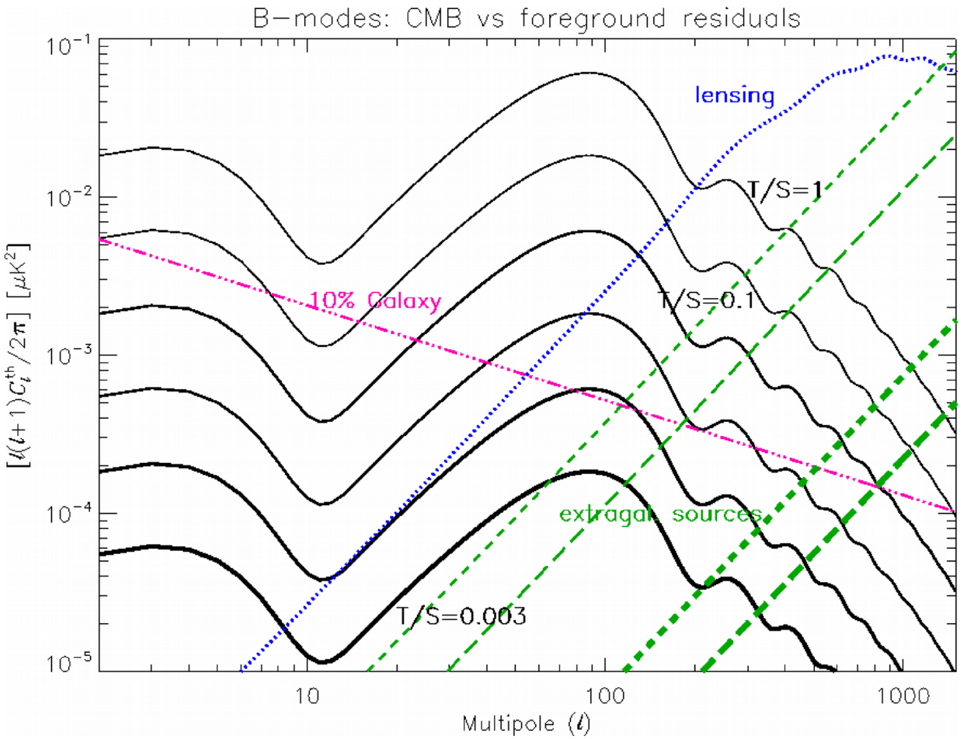

Massardi *et al*. 2016

Our approach

- The synchrotron signal is intrinsically linear polarized (up to ~70-80%)
- Helical magnetic field produces an intrinsic circular polarized signal (~ 0.1 %)
- Higher frequencies allow to study components closer and closer to the nucleus (p≈2-3)

$$\tau_{\mathrm{sync}} \propto B_{\perp}^{(p+2)/2} \nu^{-(p+4)/2}$$

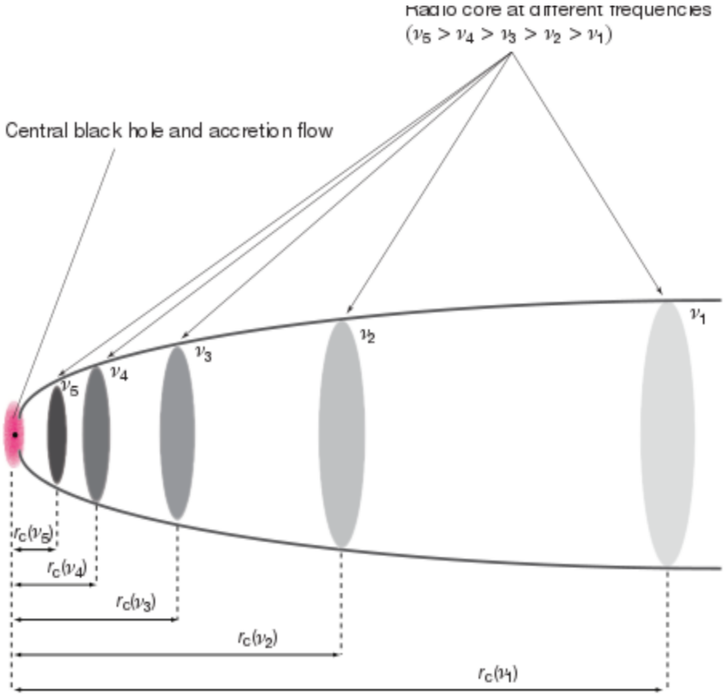

Possible (complementary) approaches:

- Very high resolution VLBI campaigns (they can cope with only few objects and are very demanding in terms of resources)
- Statistical approach: study samples of objects with (lower resolution) multi-frequency and multi-epoch polarimetry (particularly suitable to study blazars).

A biased and unconstrained picture

- Polarization properties of extragalactic radio sources at high frequencies (> 20 GHz) were still poorly constrained.

References	Frequency (GHz)	# sources	Notes
Eichendorf & Reinhardt (1979)[17]	[0.4, 15]	510	compilation of multi–frequency data
Tabara & Inoue (1980)[18]	[0.4, 10.7]	1510	compilation of multi–frequency data
Simard-Normandin *et al.* (1981)[19,20]	[1.6, 10.5]	555	compilation of multi–frequency data
Perley (1982)[21]	1.5, 4.9	404	compilation of multi–frequency data
Rudnick *et al.* (1985)[22]	[1.4, 90]	20	compilation of multi–frequency data
Aller *et al.* (1992)[23]	4.8, 8.0, 14.5	62	90% complete sample with $S_{5\,\mathrm{GHz}} > 1.3\,\mathrm{Jy}$
Okudaira *et al.* (1993)[24]	10	99	flat-spectrum sources with $S_{5\,\mathrm{GHz}} > 0.8\,\mathrm{Jy}$
Nartallo *et al.* (1998)[25]	273	26	compilation of flat-spectrum radio sources
Condon *et al.* (1998) - NVSS[26]	1.4	$\sim 2 \times 10^6$	100% complete survey down to $S_{1.4\,\mathrm{GHz}} > 2.5\,\mathrm{mJy}$
Aller *et al.* (1999)[27]	4.8, 8.0, 14.5	41	BLLac sources
Fanti *et al.* (2001)[28]	4.9, 8.5	87	CSS sample with $S_{0.4\,\mathrm{GHz}} > 0.8\,\mathrm{Jy}$
Lister (2001)[29]	43	32	90% complete sample with $S_{5\,\mathrm{GHz}} > 1.3\,\mathrm{Jy}$
Klein et al (2003)[30]	1.4, 2.7, 4.8, 10.5	192	compilation of detections of the B3-VLA survey
Ricci *et al.* (2004)[31]	18.5	250	complete sample with $S_{5\,\mathrm{GHz}} > 1\,\mathrm{Jy}$
Jackson *et al.* (2007)[32]	8.4	~ 16000	JVAS-CLASS surveys
Massardi *et al.* (2008) AT20G-BSS[11]	4.8, 8.6, 20	320	AT20G bright sample
Lopez-Caniego *et al.* (2009)[33]	23, 33, 41	22	polarization detections in WMAP maps
Jackson *et al.* (2010)[34]	8.4, 22, 43	230	WMAP sources follow-up
Murphy *et al.* (2010) AT20G[9]	4.8, 8.6, 20	5890	93% complete survey with $S_{20\,\mathrm{GHz}} > 40\,\mathrm{mJy}$
Trippe *et al.* (2010)[35]	[80, 267]	86	complete sample with $S_{90\,\mathrm{GHz}} > 0.2\,\mathrm{Jy}$
Battye *et al.* (2011)[36]	8.4, 22, 43	230	WMAP sources follow-up
Sajina *et al.* (2011)[12]	4.8, 8.4, 22, 43	159	AT20G sources follow-up
Massardi *et al.* (2013)[37]	4.8, 8.6, 18	193	complete sample with $S_{20\,\mathrm{GHz}} > 500\,\mathrm{mJy}$
Agudo *et al.* (2014)[38]	86, 229	211	complete sample of flat-spectrum sources with $S_{86\,\mathrm{GHz}} > 1\,\mathrm{Jy}$
Farnes *et al.* (2014)[39]	[0.4, 100]	951	Compilation of multi–frequency data
Planck Collaboration (2015)[8]	30, 44, 70	122, 30, 34	polarization detections in Planck LFI maps (PCCS2)
	100, 143, 217, 353	20, 25, 11, 1	polarization detections in Planck HFI maps (PCCS2)

Compilations (no close observations at different frequencies, no completeness)

Spectral selection (no completeness)

High flux density treshold, i.e. ≈ 1 Jy (WMAP, PLANCK cat.)

Complete sample with high frequency obs.

Polarimetric observations: critical points

- Polarized signal is intrinsically highly polarized but indeed we measure **2.5% at 20 GHz**:

  for objects ~ 100 mJy in total intensity we need sub mJy sensitivities

$$\sigma_{th} = \frac{2k_B T_{sys}}{A_{eff}\left[N(N-1)\Delta\nu\,\tau P\right]^{1/2}}$$

e.g., for a 2.5 % we need a factor ~2.0x10^3 more in observing time!

- Calibration: polarimetric observations require **dedicated calibrators** (e.g. for leakage solutions and, in some cases, also an absolute characterization of the polarization angle).

- Again, **calibration recipes** are far from being complete (e.g. in Stokes V) and definitive.

- Get rid of **depolarization effects**: beam depolarization, differential Faraday rotation by electron plasma, and bandwidth depolarization

  … A multi-frequency approach also implies to cope with **variability** (which is typically higher at higher frequencies, even 10-20 % in few days): observations should be close in time to avoid related biases.

The starting point: AT20G and PACO

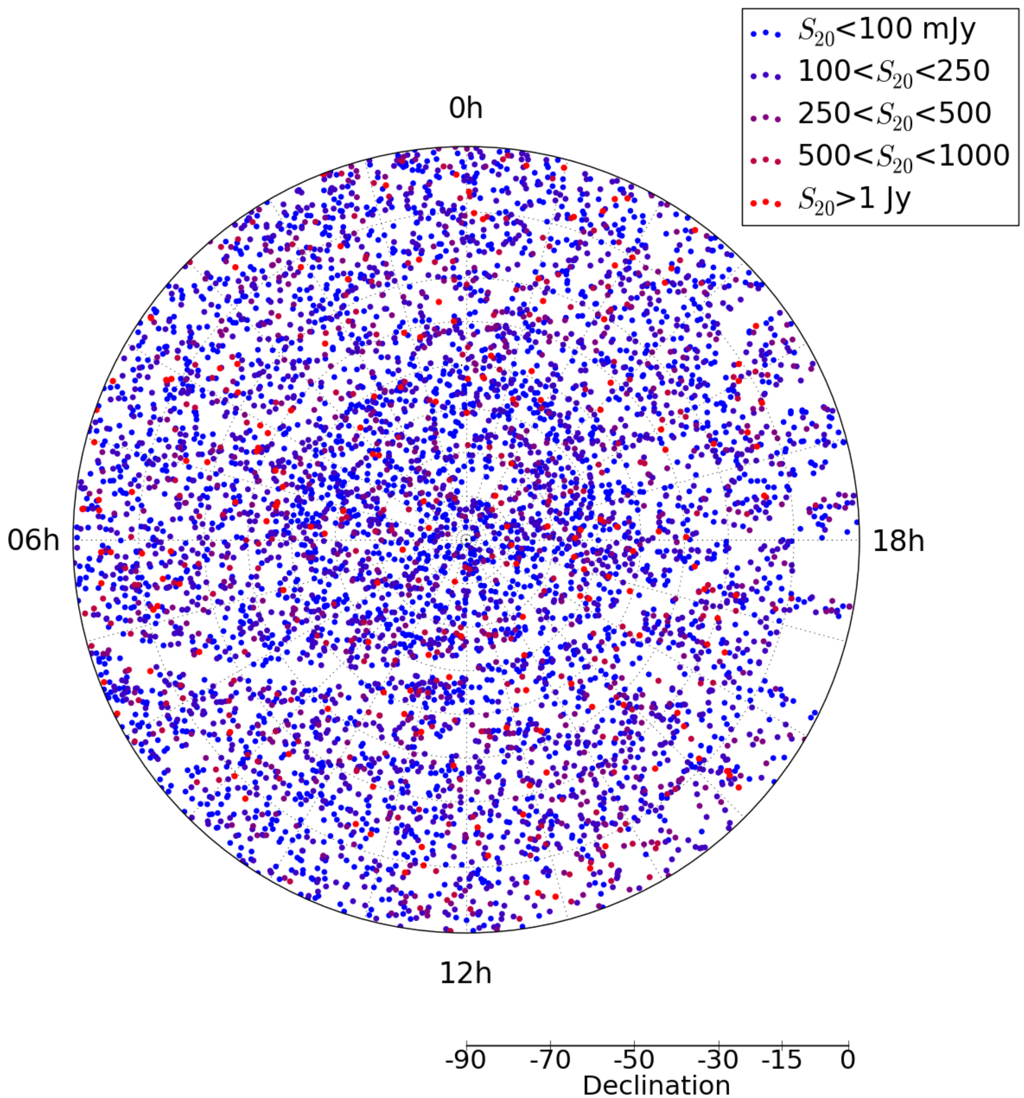

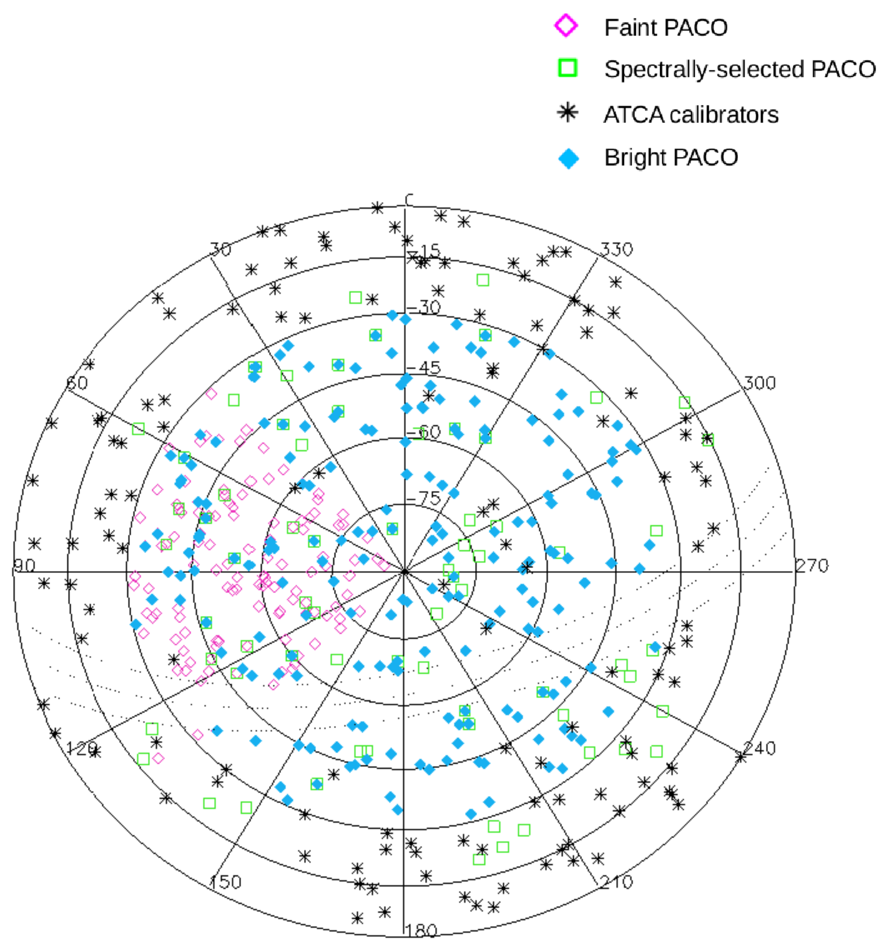

The AT20G survey (T. Murphy *et al.* 2010; M. Massardi *et al.* 2011):
5890 sources; only 768 detected in polarization at 20 GHz; only 467 have also detections at 5 and/or 8 GHz.

The PACO project (Massardi et al. 2016):
three partially overlapping sub-sample,
464 AT20G sources in total;
total intensity in the 4.5-40 GHz (ATCA) + Planck up to 217 GHz;
65 epochs between July 2009 and August 2010; more than 450 h allocated.

ATCA observations (104 faint PACO objects)

Epoch	allocated time	frequencies	# objects	region
Sep. 2014	21 h	[5.5;38] GHz	53	b < - 75°
Mar.-Apr. 2016	26 h	[5.5;38] GHz	51	-75° ≤ b < -65°
	14 h	2.1 GHz	104	b < - 65°
July 2016*	5 h	33-35 GHz	35	b < -75°

- Spatial configuration: H214 (hybrid configuration). Resolution $\lambda/b_{max}\approx 5\div 90$ arcsec (without CA06).(*H75)
- Integration on source: at least 3 min (e.g. 2X1.5 min, at least 2 cuts at different hour angles).
- Sensitivity: ≈ 0.6 mJy (≈ 1 mJy for 2.1 GHz).

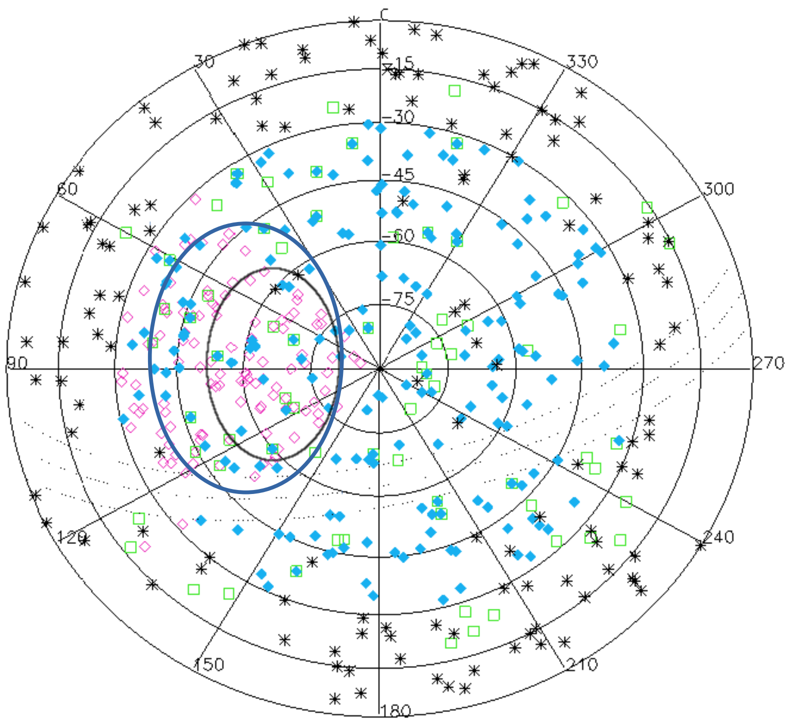

ATCA obs (Sep 2014, Mar-Apr 2016)

- Observations consider all the Stokes parameters I,Q,U,V.
- Total intensity flux I with associated error $\sigma_I = \sigma_V$ (+ 2.5% I).
- Polarized flux density:

$$P = \sqrt{Q^2 + U^2 - \sigma_V^2} \qquad \sigma_P = \sqrt{\frac{Q^2\sigma_Q^2 + U^2\sigma_U^2}{Q^2 + U^2}} \text{ (+10\% P)}$$

  - Overall detection rate in polarimetry is about **90% at 5 σ.**

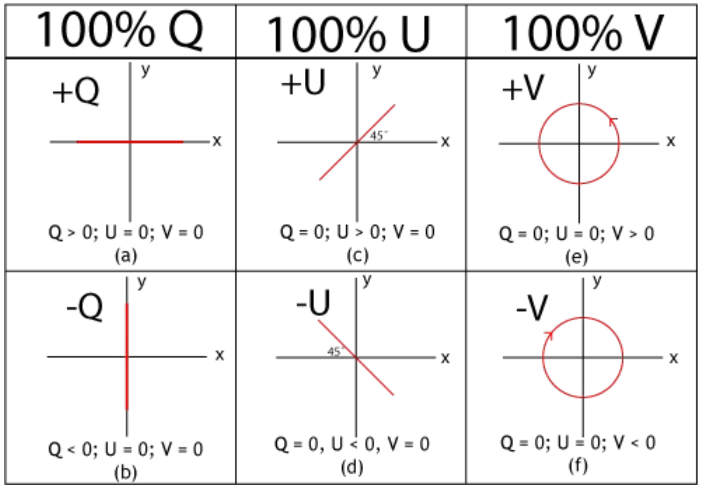

- Double/triple power law models for fitting spectra both in I and P:
  - Total intensity: 4X512 MHz chunks;
  - Polarization: 2X1 GHz chunks.

$$S(\nu) = \frac{S_0}{\left(\frac{\nu}{\nu_0}\right)^{-a} + \left(\frac{\nu}{\nu_0}\right)^{-b}}$$

  - Success rates:

    94% total intensity ($\chi^2 \approx 1.12$);

    75% polarization ($\chi^2 \approx 1.89$).

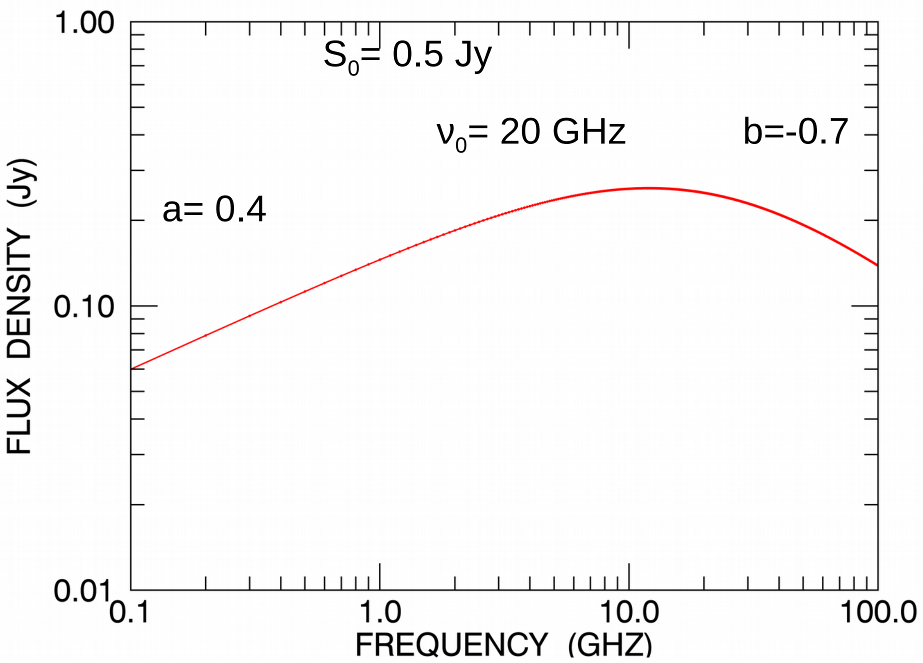

ATCA obs (Sep 2014, Mar-Apr 2016)

Spectra in total intensity and polarization; pol. fraction and PA

(error bars are smaller than plot symbols)

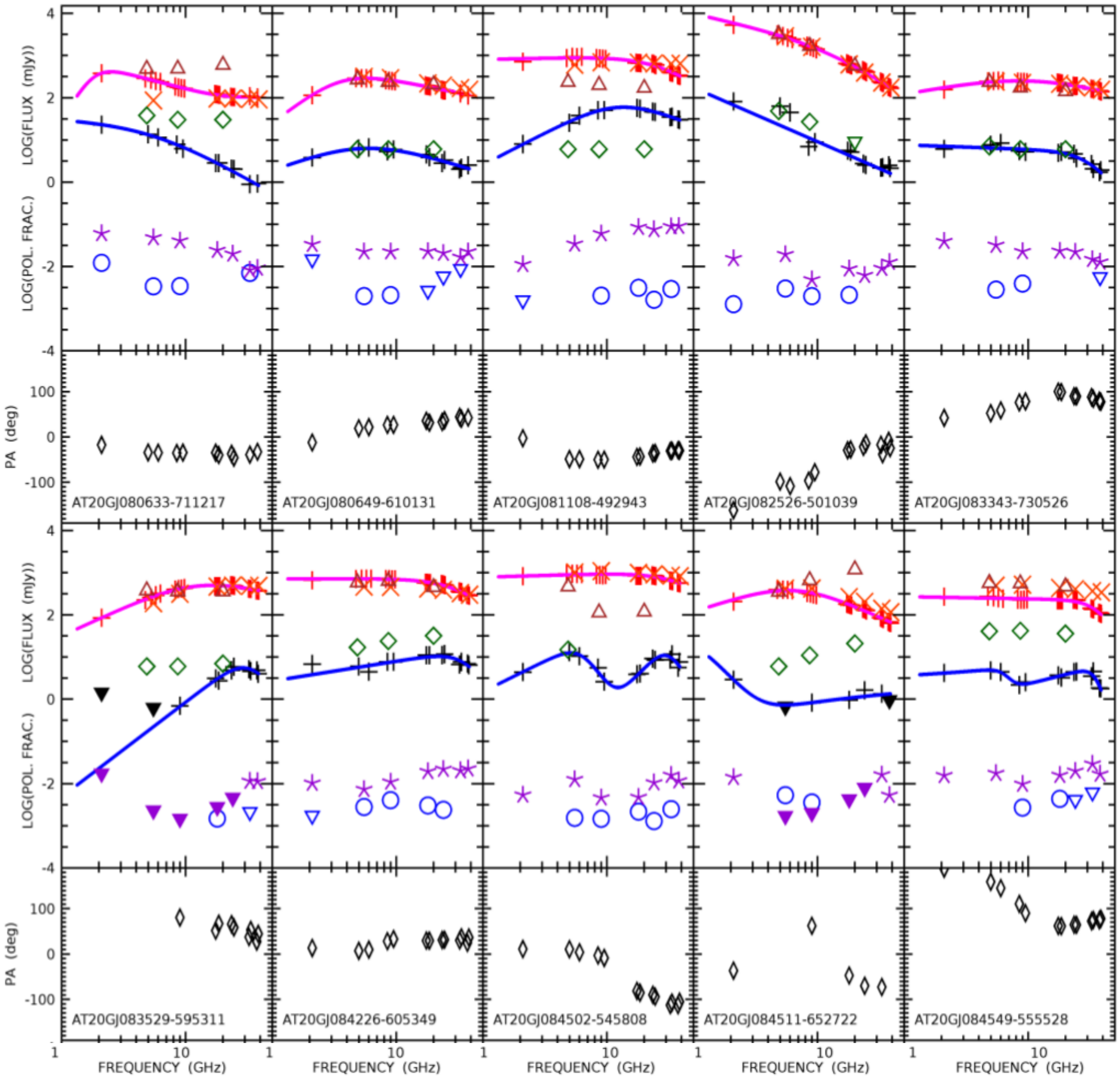

+ Tot. int.
+ Pol.
▼Upper limits Pol.
Δ Tot. Int. AT20G (best epoch in 2004-2008)
◊ Pol. AT20G (best epoch in 2004-2008)
x Tot. int. PACO (Jul 2009-Aug 2010)
– Tot. int. fit curve
– Pol. fit curve
* (Linear) Pol. fraction
○ (Circular) Pol. fraction
◊ Polarization Angle

Colour-colour plots

(error bars are smaller than plot symbols)

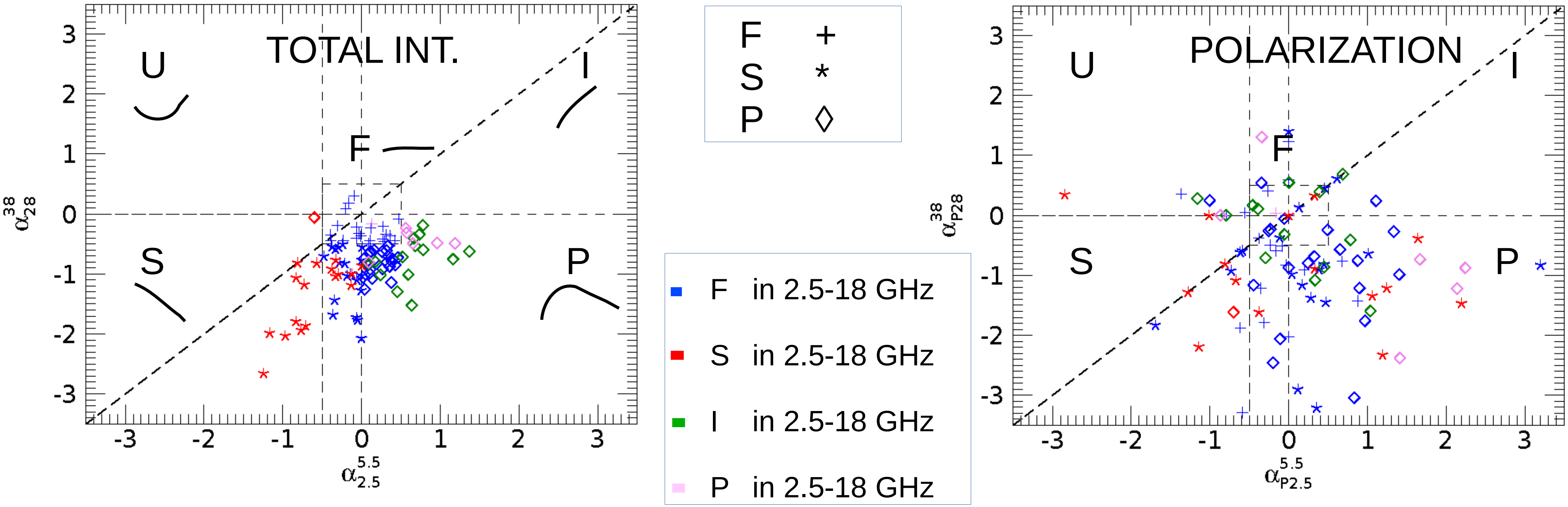

The changing behaviour is also found in analysis of AT20G results

Here we use fit and extend up to 38 GHz with an higher detection rate.

Tot. Int. → Pol. Int. ↓	(I)	(P)	(F)	(S)	(U)	
(I)	0	3	0	1	0	4
(P)	0	24	4	20	0	48
(F)	0	5	4	4	0	13
(S)	0	5	8	7	0	20
(U)	0	8	5	3	0	16
(NA)	0	1	1	1	0	3
	0	46	22	36	0	

PACO results in tot. intensity confirmed.

We add polarization.

TOT. Int.	2.5 – 5.5 GHz	5.5 – 10 GHz	10 – 18 GHz	18 – 28 GHz	28 – 38 GHz
All	−0.02	−0.11	−0.24	−0.46	−0.75
Steep	−0.33	−0.37	−0.46	−0.76	−1.02
Peaked	0.32	0.06	−0.14	−0.42	−0.74
Flat	−0.01	−0.12	−0.14	−0.26	−0.34

POL. Int.	2.5 – 5.5 GHz	5.5 – 10 GHz	10 – 18 GHz	18 – 28 GHz	28 – 38 GHz
All	0.15	−0.06	−0.15	−0.53	−0.80
Steep	0.33	−0.06	−0.24	−0.76	−0.92
Peaked	0.49	−0.01	−0.06	−0.32	−0.73
Flat	−0.21	−0.29	−0.33	−0.54	−0.68

MWA + ATCA

(Galluzzi et al. 2017, Hurley-Walker et al. 2016)

$\alpha_{0.2}^{0.4}$, $\alpha_{2.5}^{5.5}$, and α_{28}^{38}

Synchrotron comps.

Polarization is crucial to assess # components in ~50% cases.

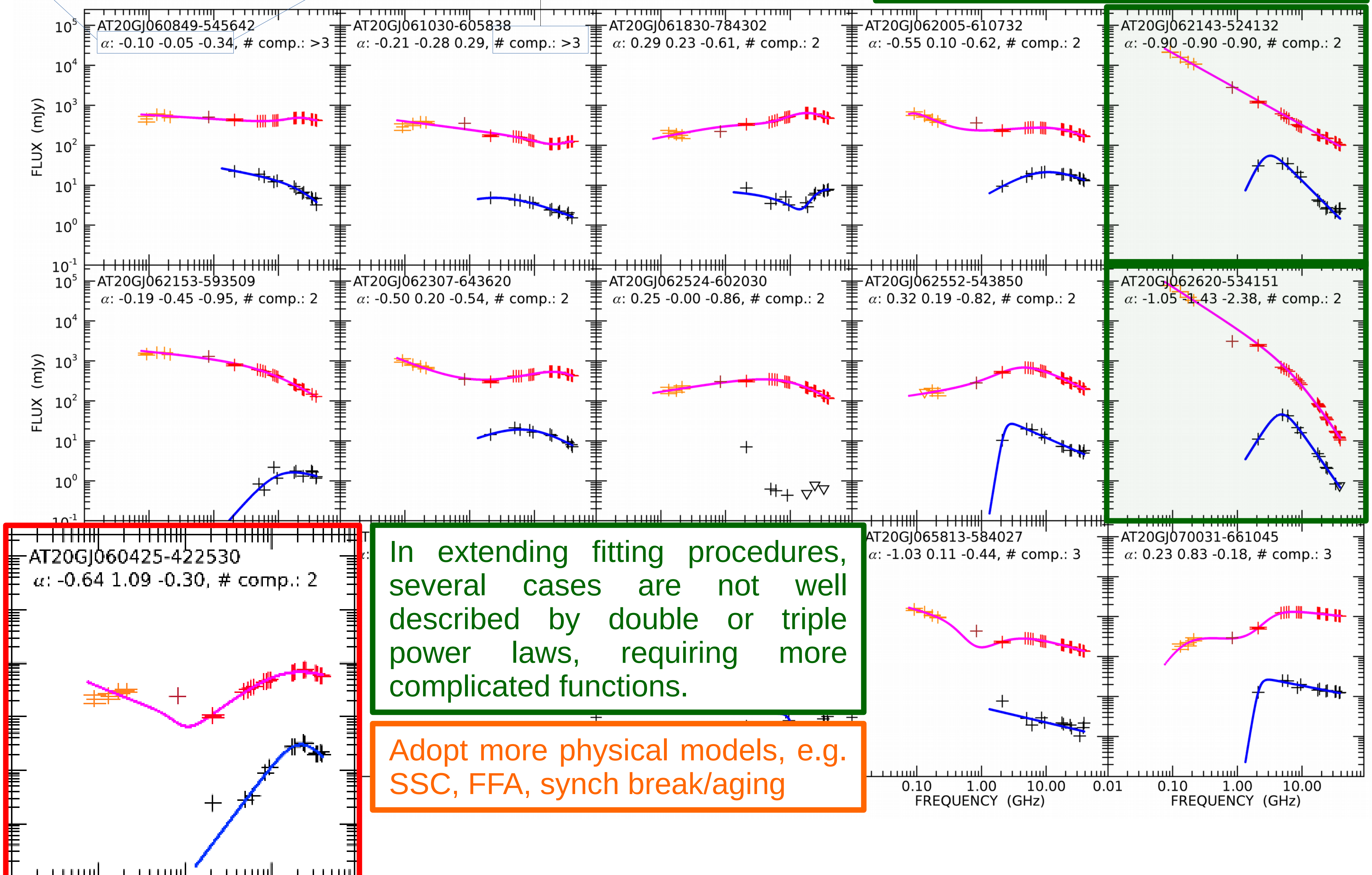

In extending fitting procedures, several cases are not well described by double or triple power laws, requiring more complicated functions.

Adopt more physical models, e.g. SSC, FFA, synch break/aging

ALMA Data

(Galluzzi et al. 2019)

- Observed proposal for ALMA-Cycle 3 to measure the polarization of the PACO faint sample at 100GHz to even higher sensitivity (down to 0.03 mJy) .
- Only 32 sources selected from the original 53 (obs. in Sep. 2014) drawn from the faint PACO sample.

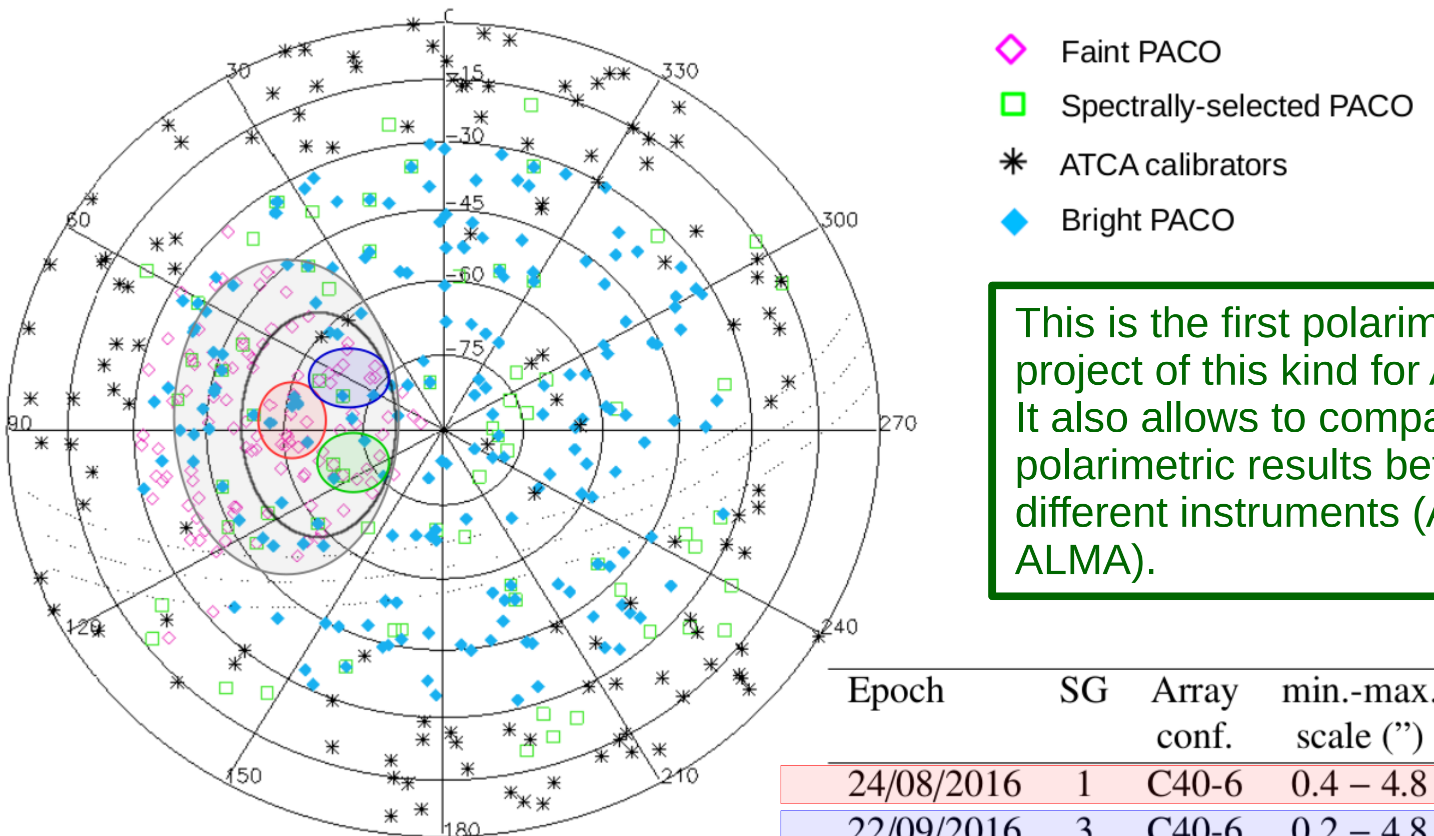

This is the first polarimetric project of this kind for ALMA. It also allows to compare polarimetric results between two different instruments (ATCA and ALMA).

Epoch	SG	Array conf.	min.-max. scale (”)	time on source (min)	th. sens. (μJy)
24/08/2016	1	C40-6	0.4 – 4.8	5.04	40
22/09/2016	3	C40-6	0.2 – 4.8	11.69	20
27/09/2016	2	C40-6	0.2 – 4.8	11.69	20

MWA + ATCA +ALMA

(Galluzzi et al. 2018,2019; Hurley-Walker et al. 2016)

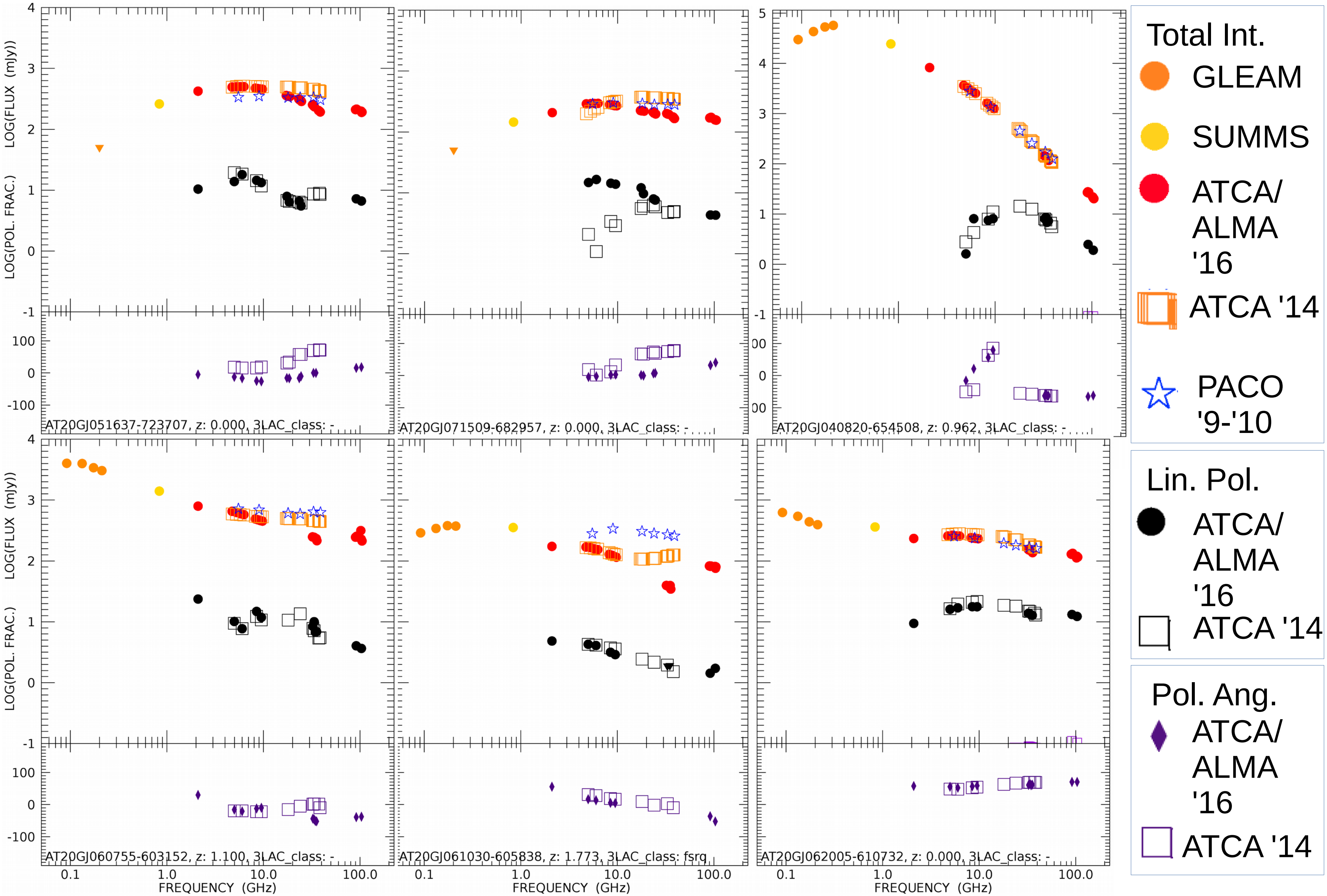

ALMA: synchrotron from the mm-core & hot spots

- PACO project didn't observe any synchrotron break up to 353 GHz, but it is unclear whether thermal dust and/or free free emissions from the host galaxy start to contribute.
- In our ALMA observations 26 out of 32 sources are somewhat in excess of expectations based on fits of the ATCA 2016 total intensity measurements. The median excess is of ∼ 40%, with a maximum of ~98%.

Polarized flux densities and angles are suggestive of genuine synchrotron emissions from (a further component) the mm-core and/or hotspots.

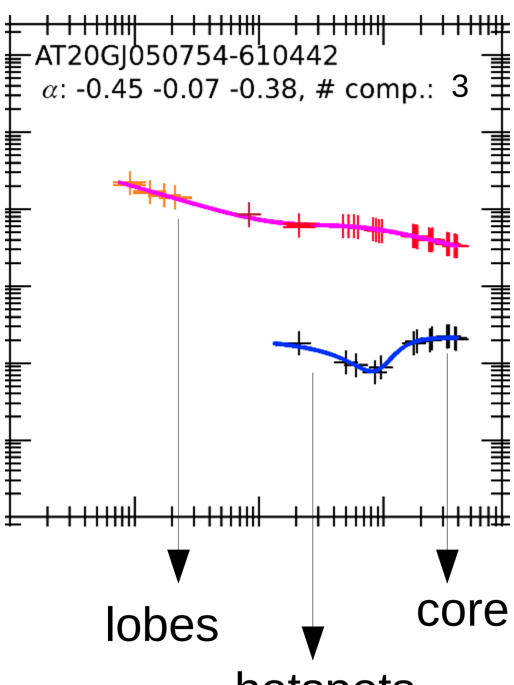

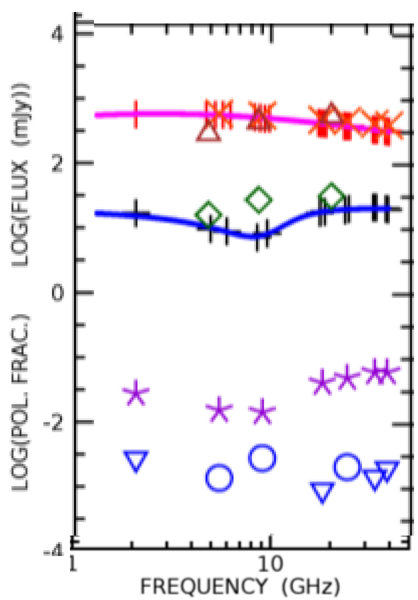

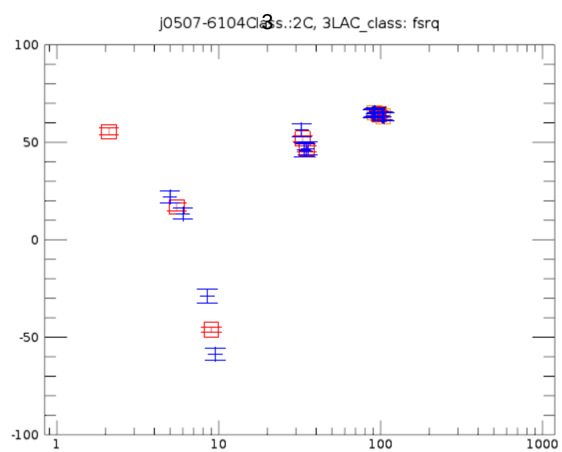

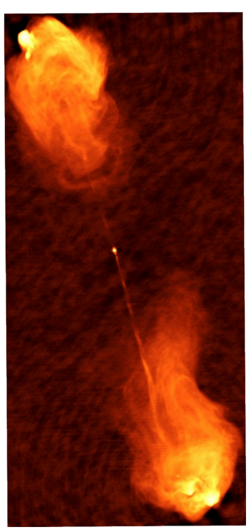

ALMA: synchrotron from the mm-core & hot spots

- PACO project didn't observe any synchrotron break up to 353 GHz, but it is unclear whether thermal dust and/or free free emissions from the host galaxy start to contribute.
- In our ALMA observations 26 out of 32 sources are somewhat in excess of expectations based on fits of the ATCA 2016 total intensity measurements. The median excess is of ∼ 40%, with a maximum of ~98%.

Polarized flux densities and angles are suggestive of genuine synchrotron emissions from (a further component) the mm-core and/or hotspots.

Exploiting ALMA capabilities in, e.g. Band 3 & 6, by selecting fainter objects (< 100 mJy) will help to address these points and to discriminate FSRQ from BLLacs. Search for breaks and arising contributions

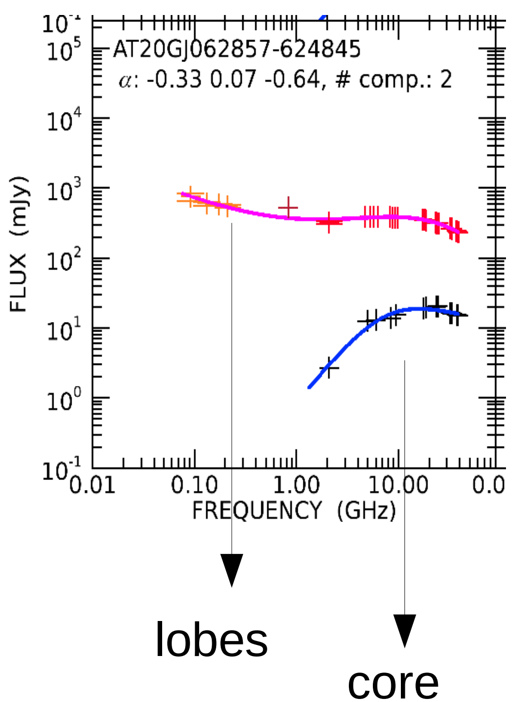

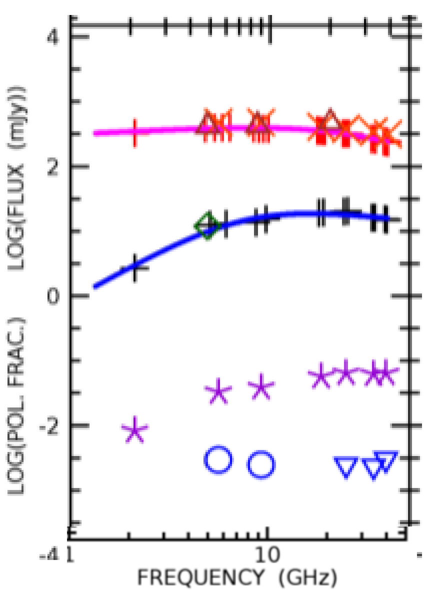

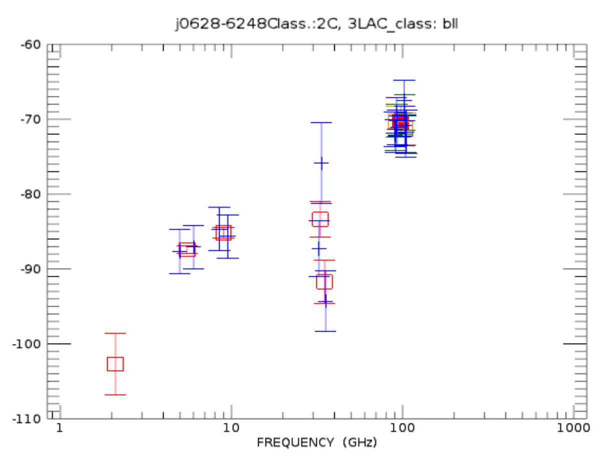

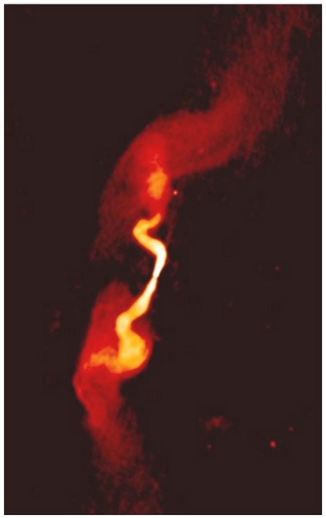

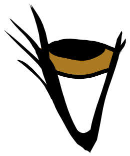

Linear polarization fractions

- Agudo et al. (2010) between 15 − 90 GHz and Sajina et al. (2011) between 5 − 40 GHz find indications of increasing polarization fraction with frequency. (Detection bias affected?)
- In principle strong Faraday depolariz. for ν < 10 GHz (but what about lobes?), higher magnetic order toward innermost regions (but what about turbulence and BLR/NLR clouds?)

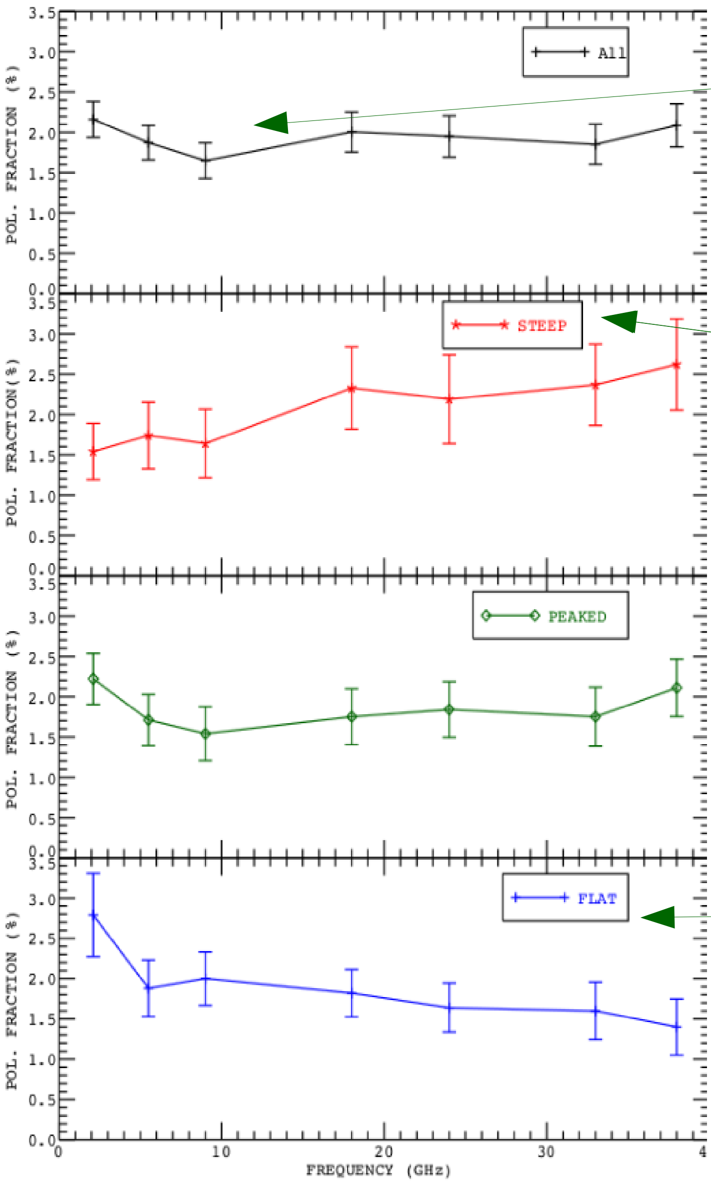

Faraday depolariz. hampered at lower frequencies by a more extended component

No statistically significant increase of the polarization fraction (just a weak trend for STEEP)

- Higher # component, higher averaging effect with increasing frequency
- High density screen of non relativistic electrons but also Faraday conversion
- Turbulence might intrinsically hamper ordered B

Weak decreasing trend for flatter objects (btw 2-3 σ). They typically show quite constant polarization angles at different frequencies.

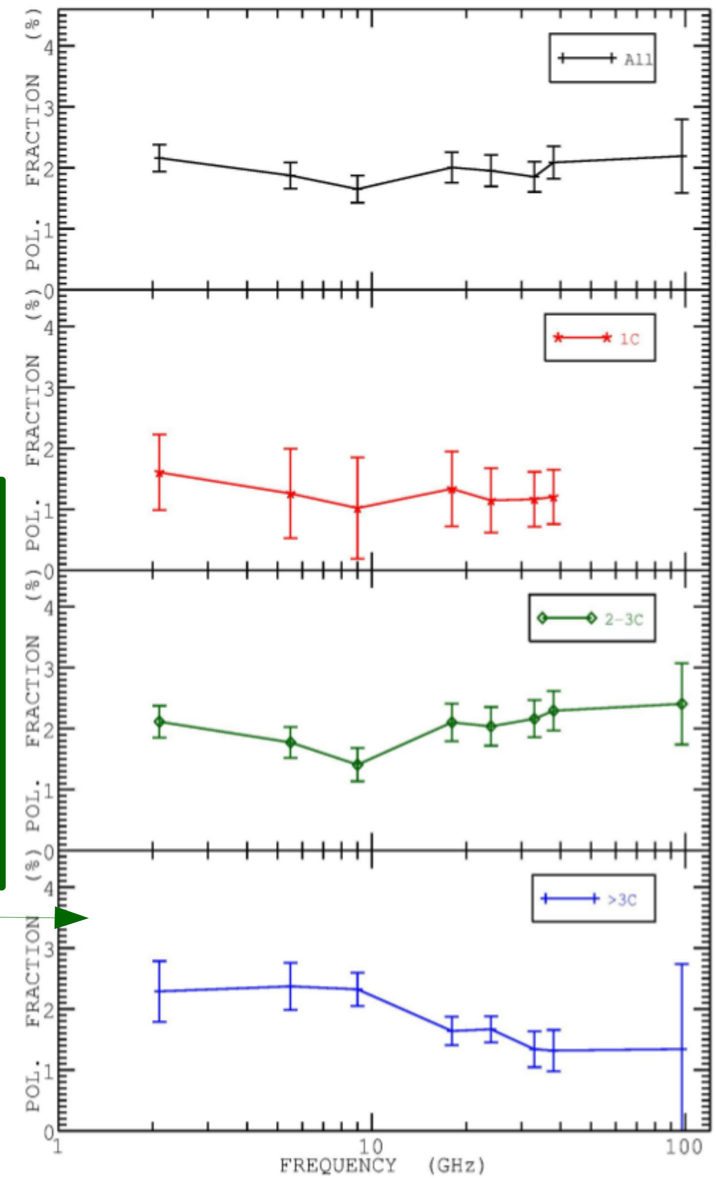

Polarization angle

Some authors report intrinsic RMs up to 1000 rad/m^2 in wideband observations up to 15 GHz. Departure from λ^2 probably due to turbulent medium.

– In the ATCA data, we identify two regimes, i.e. cm and mm-wavelenghts and perform separate linear fit

(~40% cm, ~57% mm) and find high RMs (up to 4000 rad/m^2) matching the structural complexity we argued (also consistent with the linear polarization fraction behaviour). We again found several departures from the λ^2.

1.1-10 GHz

All sample (42)			1C (3)			2-3C (31)			>3C (8)		
I	med	III	I	med	III	I	med	III	I	med	III
18	37	58	-	60	-	15	34	53	-	37	-
All sample (34)			**1C (3)**			**2-3C (24)**			**>3C (7)**		
I	med	III	I	med	III	I	med	III	I	med	III
52	100	236	-	212	-	39	77	216	141	236	259

17-39 GHz

All sample (59)			1C (4)			2-3C (50)			>3C (5)		
I	med	III	I	med	III	I	med	III	I	med	III
225	635	1397	-	342	-	283	637	1397	-	1141	-
All sample (45)			**1C (3)**			**2-3C (37)**			**>3C (5)**		
I	med	III	I	med	III	I	med	III	I	med	III
900	2615	5429	-	814	-	942	2562	5495	4010	4076	8972

$$\Delta\phi = \mathrm{RM}\lambda^2$$

$$\mathrm{RM} = \frac{e^3}{2\pi m^2 c^4}\int_0^d n_e(s)B_{||}(s)\,\mathrm{d}s$$

$$\mathrm{RM}_{\mathrm{obs}} = \frac{\mathrm{RM}_{\mathrm{AGN}}}{(1+z)^2} + \mathrm{RM}_{\mathrm{Gal}} + \mathrm{RM}_{\mathrm{ion}}$$

<z> ~ 0.94 (~70% with z)

$\mathrm{RM}_{\mathrm{Gal}}$ ~ +20 rad/m^2

$\mathrm{RM}_{\mathrm{ion}}$ < 5 rad/m^2

Polarization angle

Some authors report intrinsic RMs up to 1000 rad/m^2 in wideband observations up to 15 GHz. Departure from λ^2 probably due to turbulent medium.

– In the ATCA data, we identify two regimes, i.e. cm and mm-wavelenghts and perform separate linear fit

(~40% cm, ~57% mm) and find high RMs (up to 4000 rad/m^2) matching the structural complexity we argued (also consistent with the linear polarization fraction behaviour). We again found several departures from the λ^2.

– ALMA data (although big uncertainties ~ 1/λ^2) reveal a bunch of objects with extreme intrinsic RMs, again consistent with structure, enforcing indications of dense external screens.

$$\Delta\phi = \mathrm{RM}\lambda^2$$
$$\mathrm{RM} = \frac{e^3}{2\pi m^2 c^4}\int_0^d n_e(s) B_{||}(s)\,\mathrm{d}s$$

$$\mathrm{RM_{obs}} = \frac{\mathrm{RM_{AGN}}}{(1+z)^2} + \mathrm{RM_{Gal}} + \mathrm{RM_{ion}}$$

<z> ~ 0.94 (~70% with z)
$\mathrm{RM_{Gal}}$ ~ +20 rad/m^2
$\mathrm{RM_{ion}}$ < 5 rad/m^2

1.1-10 GHz

All sample (42)			1C (3)			2-3C (31)			>3C (8)		
I	med	III	I	med	III	I	med	III	I	med	III
18	37	58	-	60	-	15	34	53	-	37	-
All sample (34)			1C (3)			2-3C (24)			>3C (7)		
I	med	III	I	med	III	I	med	III	I	med	III
52	100	236	-	212	-	39	77	216	141	236	259

17-39 GHz

All sample (59)			1C (4)			2-3C (50)			>3C (5)		
I	med	III	I	med	III	I	med	III	I	med	III
225	635	1397	-	342	-	283	637	1397	-	1141	-
All sample (45)			1C (3)			2-3C (37)			>3C (5)		
I	med	III	I	med	III	I	med	III	I	med	III
900	2615	5429	-	814	-	942	2562	5495	4010	4076	8972

90-105 GHz

All sample (8)	2-3C (6)	>3C (2)
1.3×10^4	1.2×10^4	3.3×10^4
All sample (5)	2-3C (3)	>3C (2)
1.3×10^5	6.3×10^4	1.4×10^5

Source counts

- The radio source population source counts are poorly constrained at higher frequencies (20 GHz)
- Source counts typically distinguish between steep (non-beamed objects), FSRQs and BLLac objects.
- The state-of-art models models for radio source populations are the upgraded Bonato et al. 2017 (for ν< 10-15 GHz), De Zotti et al. 2005 and Tucci &Toffolatti 2011 (for ν > 10-15 GHz)

- We provide distributions of the polarization fractions, e.g. 20 and 97.5 GHz
- We didn't find any correlation between the polarization fraction and the total flux density, i.e. P is independent from I
- We provide source counts up to 100 GHz in polarization down to mJy level (deeper than available so far) without extrapolations.

- Require deeper (blind survey mode) observations to constraint polarimetric properties of steep population at higher frequencies

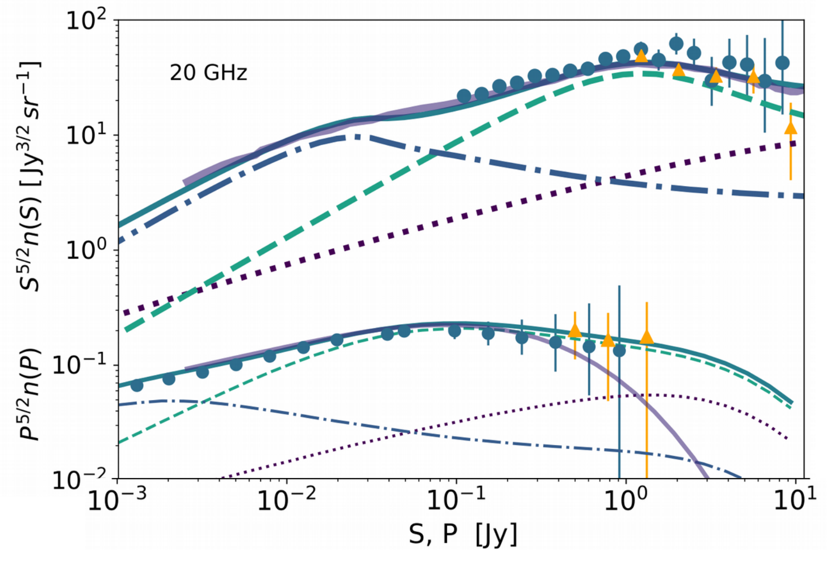

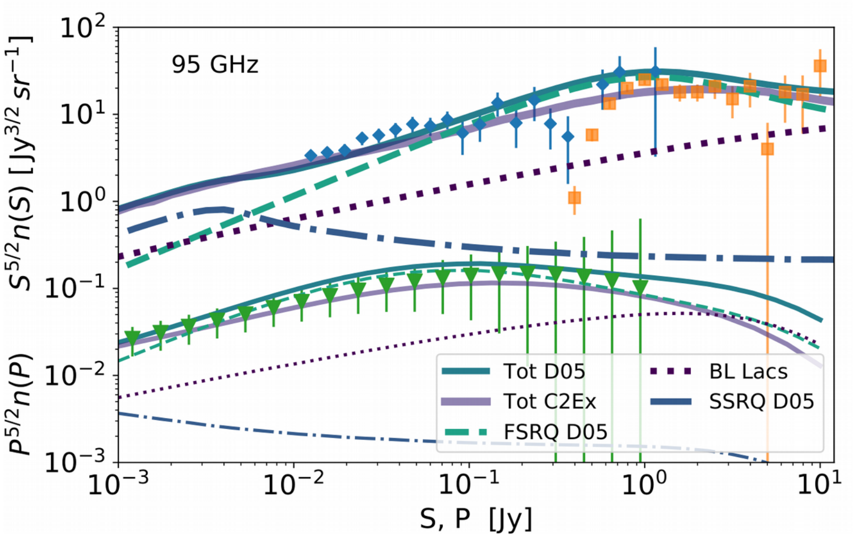

$$f(\Pi) = \text{const} \cdot \frac{1}{\sqrt{2\pi}\sigma\Pi} \exp^{-\frac{1}{2} ln^2(\Pi/\Pi_m)/\sigma^2}$$

$$\Pi = 100 \times m = 100 \times \frac{P}{I}\ (\%)$$

$$n(P) = \int_{S_0=P}^{\infty} \mathcal{P}\left(m = \frac{P}{S}\right) n(S) \frac{dS}{S}$$

Forecast for ERS foreground

(in collaboration with G. Puglisi, SISSA, [Puglisi, Galluzzi et al. 2018])

- The stochastic background of GW induced by inflation is expected to leave its footprint in CMB angular power spectrum (primordial B modes), still undetected.
- Current upper limit on r is 0.07 at 95% c.l. (BICEP 2/Keck and Planck Collaboration 2015)
- For r down to 0.001, Extragalactic Radio Sources (ERS) are important contaminant for the CMB angular power spectrum for l > 50 up to 150 GHz

- Given current and next-coming CMB experiments we forecast ERS contamination to the CMB B-mode angular power spetrum (Point Source ForeCast, PS4C)*

	Frequency [GHz]	Sensitivity [μK arcmin]	FWHM	f_{sky}
QUIJOTE	11,13,17,19	1800	1°	50%
CMB-S2	95, 150	25,30	$3.5'$	5%
CMB-S3 SA	30, 40, 95,150	8, 6, 1, 2	1°	20%
CMB-S3 LA	30, 40, 95,150	8, 6, 1, 2	$10', 7', 3', 2'$	20%
LiteBIRD	40, 50, 60, 68, 78	53, 32, 25, 19, 15	1°	100%
	89, 100,119, 140,166	12, 15.6, 12.6, 8.3, 8.7	1°	100%
CORE150	60, 100, 145	10.6, 7.1, 5.1	$14', 8', 6'$	100%

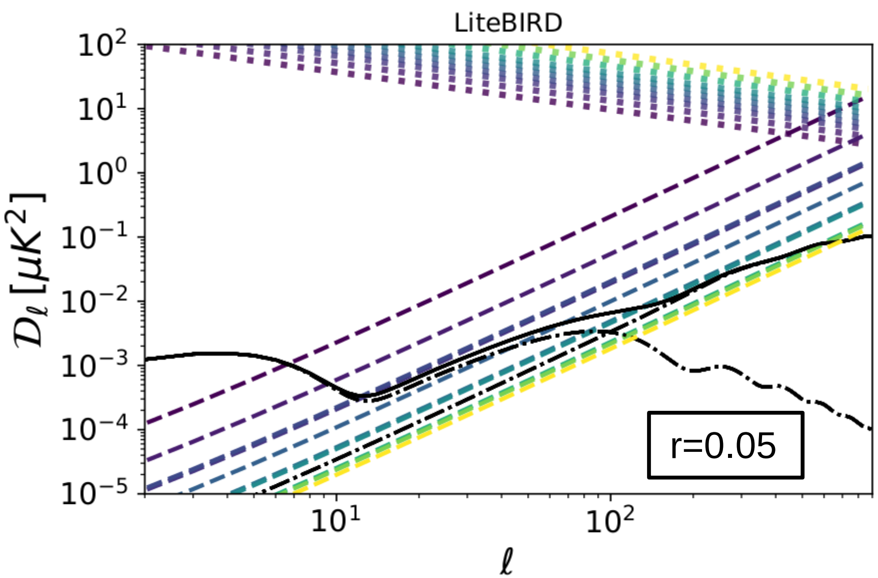

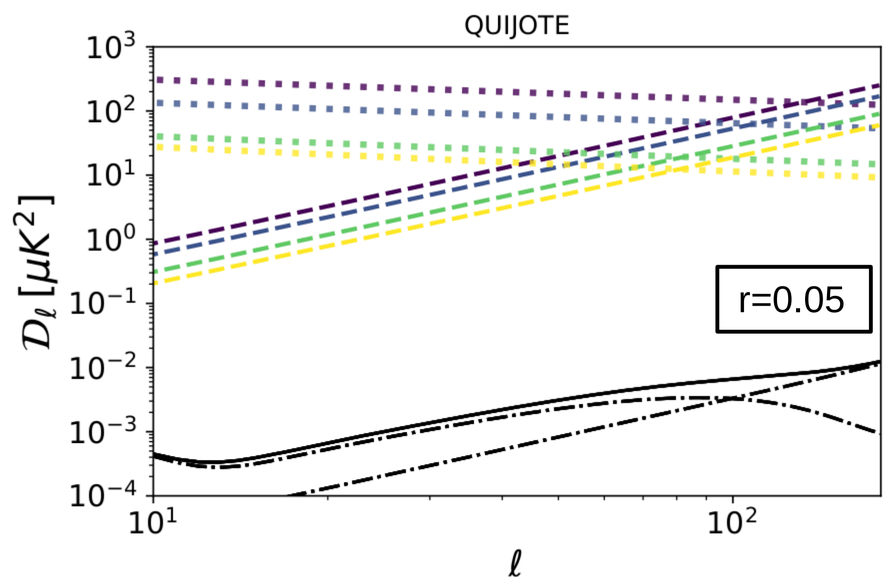

B-modes (primordial and lensed E separately)
Total B-modes
Galactic synchrotron foreground
ERS foreground
Purple to yellow → increasing frequency

* *Available at: https://gitlab.com/giuse.puglisi/PS4C*

The Tiered Radio Extragalactic Continuum Simulation

(T-RECS, PI: A. Bonaldi, SKA Organization [Bonaldi et al. 2018])

- T-RECS relies on a P-Millennium simulation with Planck Cosmology
- Very high particle resolution (1.061 x $10^8 h^{-1} M_\odot$), small box size (800 $(Mpc/h)^3$), maximum field of view 5x5 sqdeg out of z=8 with clustering
- By assuming the state-of-art models for AGNs and SFGs it provides catalogues between 150MHz and 20 GHz with morphological parameters (e.g. orientation with respect to the line of sight and size)

- We contributed with polarization modelling for AGNs, simulated catalogues validation and comparison with results in literature

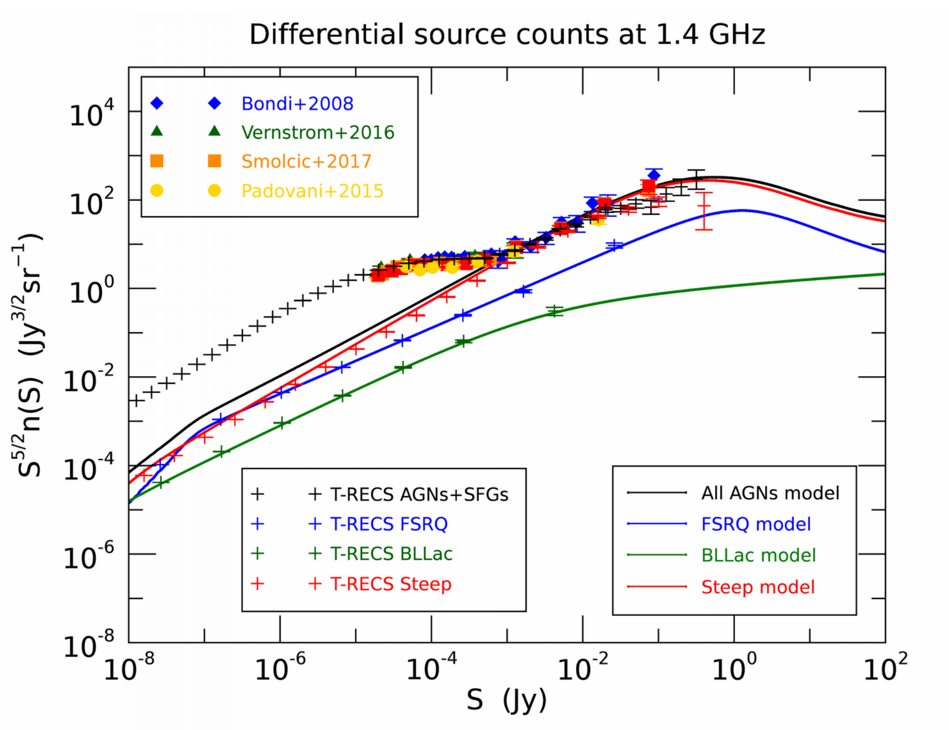

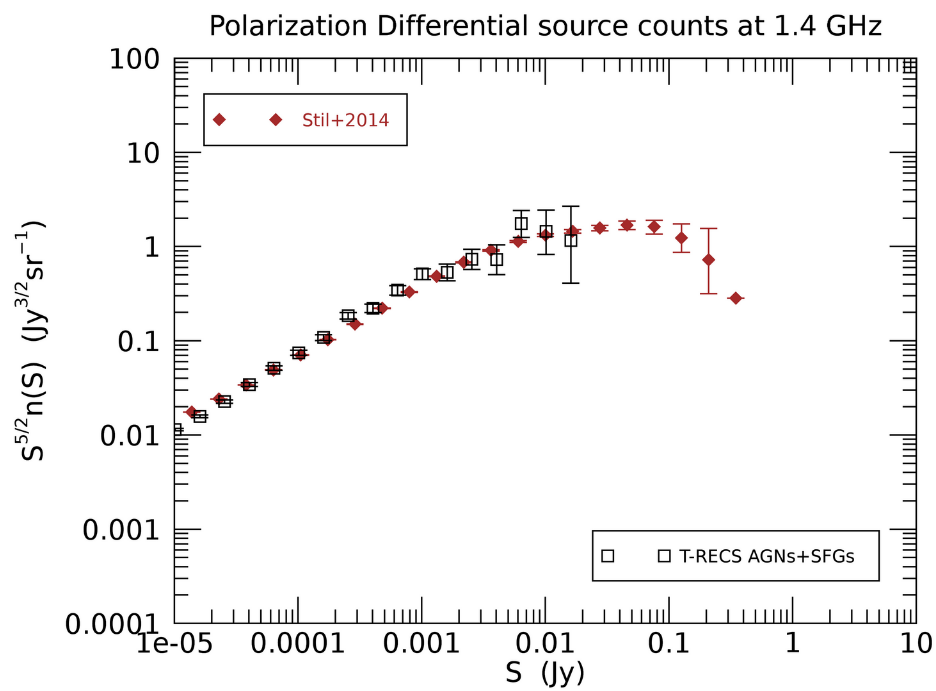

Conclusions

Thanks to high sensitivity ($\sigma_P \approx$ 0.6 mJy/beam) multi-frequency polarimetric observations of a complete sample of 104 extragalactic radio sources (det. Rate ≈ 90%) and the ALMA follow-up at 100 GHz or 32 objects (σ_P down to 30 μJy/beam):

- We characterize spectra in total intensity (up to slightly more than 3 decades) and polarization (up to 1.7 decades), clearly showing that cannot be simply inferred from total intensity for the great majority of sources
- We find correspondences between the spectro-polarimetric properties and radio galaxy morphology, inferring the number of synchrotron components
- No significant trend of the fractional polarization with either flux density or frequency was found, and this has been connected with physical scenarios (e.g. lobed emissions, beam depolarization, Faraday screens, turbulence)
- Evidence of Faraday screening effects in different frequency regimes, with values typically increasing with the frequency and the argued structural complexity.
- Highest detection rate for V: 38%; 5.5 GHz → (0.21+-0.02)% 9 GHz → (0.27+-0.02)%. Possible mechanisms: Faraday conversion and plasma screen inhomogeneities
- Mean variability indices increase with frequency characterized for several time lags (up to 10 yr). In polarization higher values by a factor ≈ 1.5-2 wrt total intensity. Adiabatic expansion, flaring activity and newly emitted component consistent with the argued structural complexity.
- We provide source counts up to 100 GHz in polarization down to mJy level (deeper than available so far) without extrapolations and forecasts for current and forthcoming CMB facilities